SIMULATION OF FARADAY WAVES WITH THE RELAP5-3D THERMAL-HYDRAULIC CODE

C. Frepoli* **and J. W. Fricano**
FPoliSolutions, LLC, 4618 Old William Penn Hwy, Murrysville, PA 15668, USA
*frepolc@fpolisolutions.com

F. Buschman and D. Aumiller
Bettis Atomic Power Laboratory, West Mifflin, PA 15122

ABSTRACT

Faraday waves result when a liquid layer is subjected to a uniform external oscillation in the vertical direction. Based on the frequency and the amplitude of the forcing oscillation, standing waves will develop. When a sinusoidal forcing function is applied to an inviscid liquid layer the Faraday wave problem reduces to a Mathieu equation. The instability evolves following a sub-harmonic resonance where the frequency of the specific wave mode is half the frequency of the forcing function. The viscosity acts as a damper by increasing the required critical amplitude for the forcing function to destabilize the system and induce Faraday wave motion.

This problem has been selected by the authors as a good candidate to assess the multidimensional capabilities of thermal-hydraulic codes. This work builds upon similar analysis was performed in the past by the same author for other codes. The interest in this problem is that the onset of the instability requires a correct formulation of the multidimensional flow. Issues associated with time and space discretization can be explored with this problem. The impact of numerical diffusion can be inspected as it results in an effective artificial viscosity which can be quantified from the numerical solution.

In this work, the ability of the nuclear system code RELAP5-3D to predict the development and behavior of these waves in a vessel downcomer geometry is assessed.

This paper is one among a series presented in this conference that illustrate the use of fundamental canonical problems to challenge key aspects of the multidimensional flow process while removing complex processes such as interfacial mass and heat transfer. The analysis evaluates whether basic criteria such as symmetry, mesh rotation invariance, wave dispersion, hydraulic instabilities, effect of gravity, etc. are predicted consistently with theoretical expectations. The Faraday wave problem is included into an automated verification suite which is described in [1] .

KEYWORDS
Faraday Wave, RELAP5-3D, Downcomer Thermal-Hydraulics

1. INTRODUCTION

A strategy to develop a comprehensive assessment of the RELAP5-3D capabilities in modeling multi-dimensional flow is presented in a separate paper at this conference [1]. Following a staged bottom-up approach of the assessment, canonical problems were identified for an initial stage of the assessment and simulated with the code.

A verification problem of interest was previously considered by one of the authors [2]. The Faraday wave problem is well suited to shed some light on the completeness of the multidimensional formulation of the subject code as well to explore the impact of numerical diffusion in 3D. Numerical diffusion is typically only analysed for simple one dimensional problems, like the classic 1D manometer problem considered in the RELAP-3D manuals [3].

Section 2 provides a brief summary of the theory behind the Faraday wave problem. More extensive literature on this topic can be found in [2] and [4]. Section 3 describes the modeling strategy considered with RELAP5-3D while results are discussed in Section 4.

2. FARADAY WAVES THEORY

A linear inviscid assumption leads the free surface boundary condition to a Mathieu Equation, [5]. The amplitude equation for an annular downcomer geometry was derived in Appendix B [4]. The wave amplitude is governed by the Mathieu Equation:

$$\frac{d^2a}{d\tau^2}+\left(p-2q\cos 2\tau\right)a=0 \tag{1}$$

Where a is the dimensionless amplitude of the wave, and p and q are the scaled (dimensionless) wave frequency and the scaled amplitude of the forcing function, respectively:

$$p_m=\left(\frac{\omega_m}{\Omega/2}\right)^2 \tag{2}$$

$$q_m=2Ak_m\tanh(k_mH) \tag{3}$$

A is the amplitude of the forcing function. Also the following definitions apply:

ω_m = Wave frequency of the mode m, characterized by the wave number k_m [rad/s]

Ω = Frequency of the forcing function (vertical oscillation) [Hz]

$\tau=\frac{\Omega t}{2}$ = Scaled time [-]

H = Initial depth of the liquid layer [m]

The frequency of the wave ω_m is related to the wave number k_m by the following relationship:

$$\omega_m^2=k_m g\cdot\tanh\left(k_mH\right) \tag{4}$$

Equation (4) is consistent with Equation 2.15 of [5] where the effect of the surface tension (capillary waves) is neglected based on the geometry of this problem.

The geometry considered is an annular downcomer with an average circumference of 14.5 m. This geometry is similar to the downcomer of the UPTF test facility [6], which is a full scale representation of

a German-design 4-loop Pressurized Water Reactor (PWR). The outside radius is 2.31 m and the inside radius is 2.06 m. The gap (the distance between the inner and outer radii of the annulus) is 0.25 m. The dominant sloshing mode wave number, k_0 in the annulus was estimated assuming a wave length equal to the average circumference of the downcomer:

$$\lambda_0 = 14.5m \tag{5}$$

Thus:

$$\begin{aligned} k_0 &= 0.433m^{-1} \\ \omega_0 &= 2.035\frac{rad}{s} \\ f_{FW,0} &= \frac{\omega_0}{2\pi} = 0.324Hz \end{aligned} \tag{6}$$

The stability chart for the inviscid solution is reproduced in Figure 1. Note that the sub-harmonic resonance discussed previously is represented by the unstable region closest to the origin.

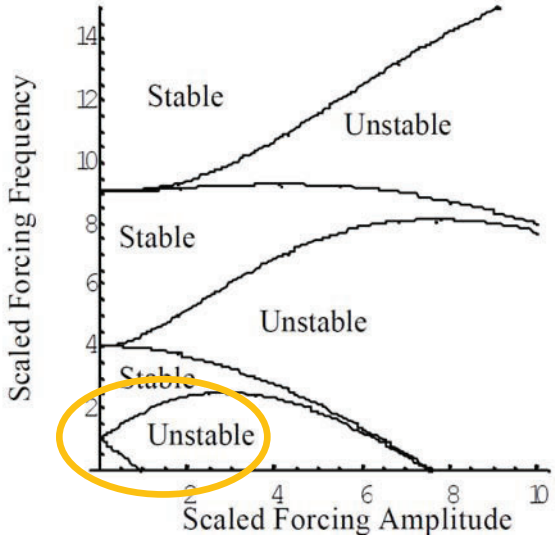

Figure 1 – Stability chart for the inviscid solution

In Figure 1 above, the scaled forcing frequency is represented by *p* whereas the scaled forced amplitude is *q*. As a result, the resonance frequency for the first mode (m=0) is given by the point which is always unstable (q=0):

$$p_0 = 1.0 \tag{7}$$

Which leads to:

$$f_0 = \frac{\Omega_0}{2\pi} = \frac{\omega_0}{\pi} = 0.648Hz$$
$$\mathrm{T}_0 = \frac{1}{f_0} = 1.544s \tag{8}$$

The circle in Figure 1 highlights the stability boundary for the sub-harmonic resonance, which is the most unstable mode. The theory also predicts higher order resonance modes, but those are not considered in this study.

The role if viscosity is discussed by Ohkawa [4]. More on this topic can also be found in the review by Benjamin and Ursell [7]. Figure 3 of Muller [7] shows that a forcing function with a non-zero critical amplitude is needed to excite the sub-harmonic oscillation. The results from Benjamin and Ursell are reproduced below in Figure 2 for convenience.

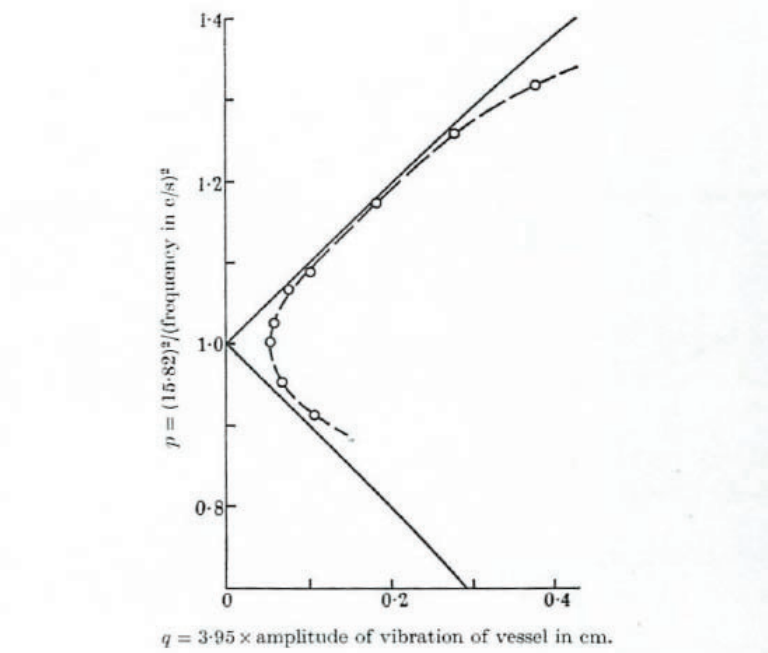

FIGURE 3. Experimental (- - -) and theoretical (—) stability curves for the (2, 1) mode in a circular cylinder of radius 2·70 cm.

Figure 2 – Reproduction of Benjamin and Ursell [7] **Figure 3**

3. SELECTED CODES AND COMPUTATIONAL MODELS

RELAP5-3D models have been created to simulate this problem. The details of the models have been constructed following the work of Frepoli [2]. This includes model geometry, the initial conditions, the boundary conditions, and the forcing function, where applicable. A schematic of the mesh is presented in Figure 3. The mesh sensitivity is assessed with three different meshes: the reference mesh is 1x12x20, a coarse variant of 1x4x20, and a fine variant of 1x12x60.

The annulus is partially filled with water to establish a level at approximately half height of the annulus. Liquid flow is injected and extracted uniformly at the bottom and a constant pressure set at the top boundary. The liquid velocity at the bottom boundary is set as:

$$v_{in}(t) = A\Omega \cos(\Omega t) \tag{9}$$

Each simulation includes three phases. The problem is allowed to run for a short time, to achieve steady conditions, before the forcing function is applied. The forcing function is then applied for some time before being disabled. The last phase is needed to observe the damping of the sloshing motion. A variant sloshing case is evaluated to establish the natural frequency predicted by the code and the predicted damping rate once the forcing function stops. Other sensitivity studies considered are the effects of the amplitude and frequency of the forcing function. These studies allow the determination of the predicted stability boundary in the Mathieu graph.

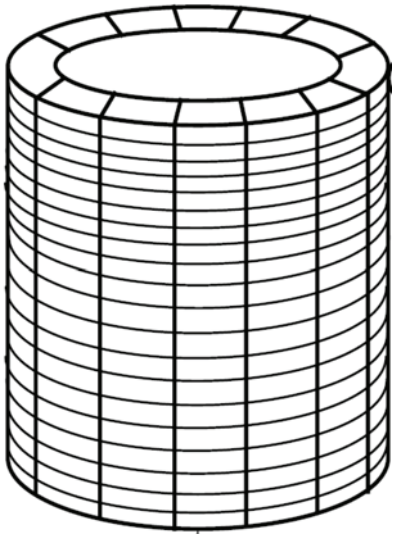

Figure 3 - Noding for an Annular Model [2]

4. SELECTED RESULTS

The reference case (Case 1021) results are presented in Figure 4 and Figure 5. The forcing frequency is set to 0.5 Hz, which is twice the natural frequency of the k_0 mode as predicted by RELAP5-3D which is found to be underestimating the theoretical value. Figure 4 shows that the resonance develops at about 40 seconds into the transient. Contrary to theoretical predictions, the code shows the instability to develop only for relatively large amplitudes of the forcing oscillation (about 0.5 m). This is associated with the artificial viscosity (numerical diffusion). This issue is also discussed by the work of Frepoli [2], Figure 4 provides a visual representation of the wave oscillation in a Lagrangian frame of reference (on the right), i.e., in a moving frame that follows the forcing function:

$$y_{wave}(t) = y_{CLL}(t) - A\sin(\Omega t) \tag{10}$$

Where y_{CLL} is the collapsed liquid level.

Figure 5 shows that the wave profile corresponds to the fundamental (m=0) sloshing mode in the annulus with a 1D standing wave with a wavelength λ, corresponding to the circumference of the annulus

(14.5 m). The wave grows to an amplitude of about 0.5 m which is about the amplitude of the forcing function in this case.

Once the forcing function is stopped, the wave is damped and the damping factor can be estimated assuming the damping is exponential, i.e., it follows the $e^{-\gamma t}$ law. The damping factor, γ, was estimated to be 0.055 sec^{-1}. As presented by [4] the damping factor can be related to the apparent viscosity experienced by the code. With ν being the kinematic viscosity, from the damping factor, γ, and the wave number *k*, the effective viscosity is computed as follows:

$$\nu = \frac{\gamma}{2k^2} = 0.147 \frac{m^2}{s} \tag{11}$$

This is about 500,000 times the physical kinematic viscosity of the fluid (water) for these conditions (saturated water at 1 bar) which is equal to $3.8 \cdot 10^{-7} \frac{m^2}{s}$. This result is similar to what is presented by Okhawa for other codes [4].

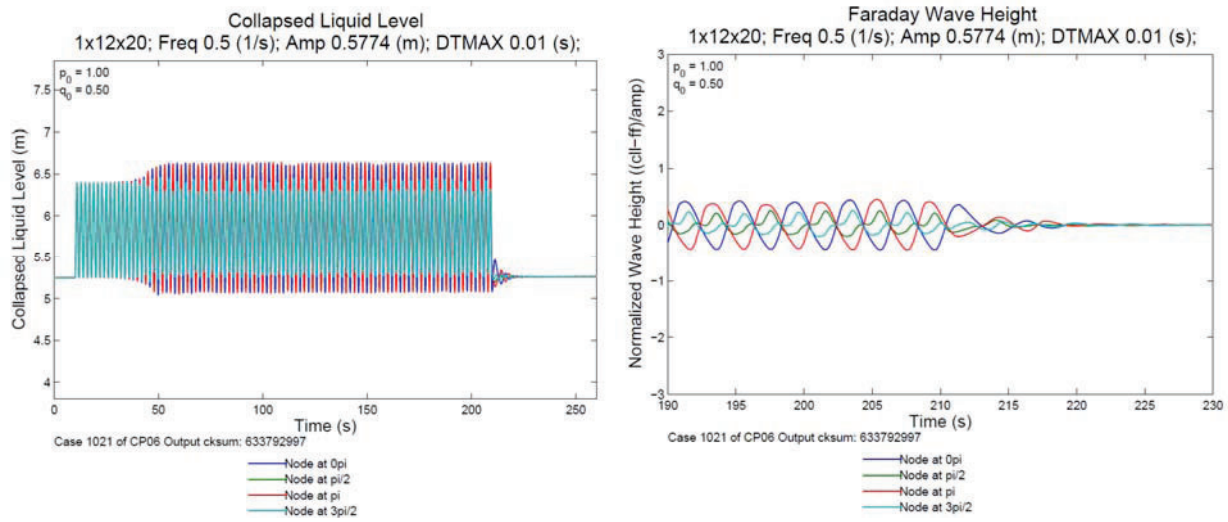

Figure 4 - Reference case (Case 1021) Collapsed Liquid Level in each of the four quadrants (Θ-coordinate) (on the left) and Faraday wave height (on the right)

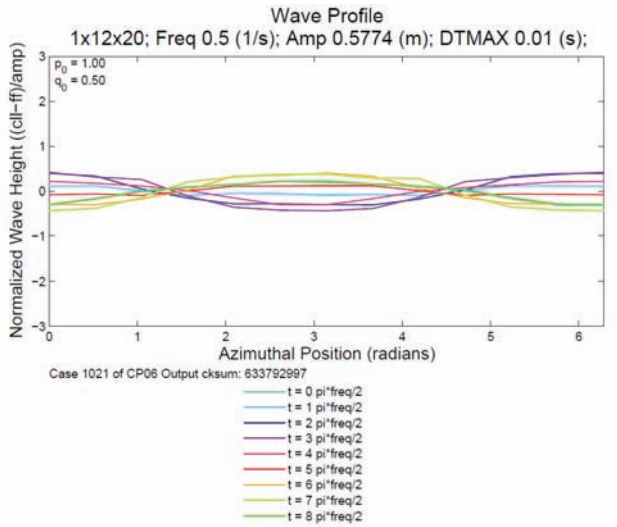

Figure 5 - Reference case (Case 1021) Faraday wave profile

The analysis is continued by assessing the capability of the code to predict the transition from stable to unstable regimes consistent with the Mathieu chart as presented in Figure 6. A total of 121 cases covering a range of forcing function frequency and amplitude values were performed. The conditions for which the wave develops were identified and plotted as blue and red circles in Figure 6.

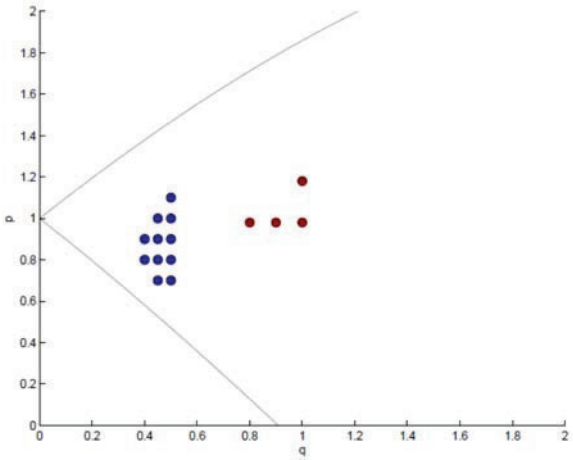

Figure 6 – Mathieu stability chart (in blue the k_0 modes and in red the k_1 modes)

4.1 Space and Time Discretization Studies

Two mesh sensitivity cases are evaluated for comparison to the reference case 1021 based on the 1x12x20 mesh. Case 1020 considers a coarsening of the azimuthal mesh, Θ, (1x4x20) and Case 1025 is a refinement of axial mesh, Z, (1x12x60).

Results are presented in Figure 7 and Figure 8. Case 1020 is similar to case 1021. The code predicts a similar wave amplitude once the motion is established and the wave profile is a clear indication of the *m=0* standing wave motion. The damping factor was estimated to be γ=0.136 for Case 1020. As observed in Figure 9, the 1x4x20 mesh damps similarly to the 1x12x20 mesh, possibly a little faster. This result is consistent with the analysis by Ohkawa [4], which states that the numerical diffusion should increase with

mesh size. However the change in magnitude of the damping factor in this case may not be significant enough to reach this conclusion.

It is worth noting that the coarse mesh, with only 4 azimuthal nodes, was sufficient to represent the wave motion. The result is consistent with the results presented by Frepoli [1] at this conference which state that in order to capture wave motion, the maximum node size in the direction of the sloshing should be a quarter of the wavelength.

The effect of the mesh in the vertical direction was assessed with Case 1025 (1x12x60). Figure 7 (on the right) shows that the solution is rather chaotic and does not lead to the development of the standing wave observed for the coarser reference mesh (Case 1021). A significant mass error was reported for this case (Figure 10) which is possibly impacting the accuracy of the solution and preventing the regular wave motion from being correctly predicted.

A time step sensitivity study was conducted by reducing the maximum allowable time step size by an order of magnitude. The results are presented in Figure 11 and Figure 12. Figure 11 shows the reduced time step case, Case 1023, having a more irregular motion of the level than in the reference case, Case 1021, which is shown in Figure 5Figure 4. However Figure 12 shows that the Faraday wave is well defined. A possible interpretation is that the case with the reduced time step size will have increase numerical viscosity, which acts to stabilize the system. According to Ohkawa [4], the effective viscosity can be related to mesh size and time step by the following relationship:

$$\nu_{num,\mathrm{k}} \approx \frac{u_k \Delta x_k}{2}\left(1-c_k\right)$$
$$c_k = \frac{u_k \Delta t}{\Delta x_k} \tag{12}$$

$\nu_{num,\mathrm{k}}$ is the apparent kinematic viscosity in the direction "k" and c_k is the Courant number in the same coordinate which is proportional the time step size. The effective numerical viscosity is therefore expected to increase as the time step size decreases.

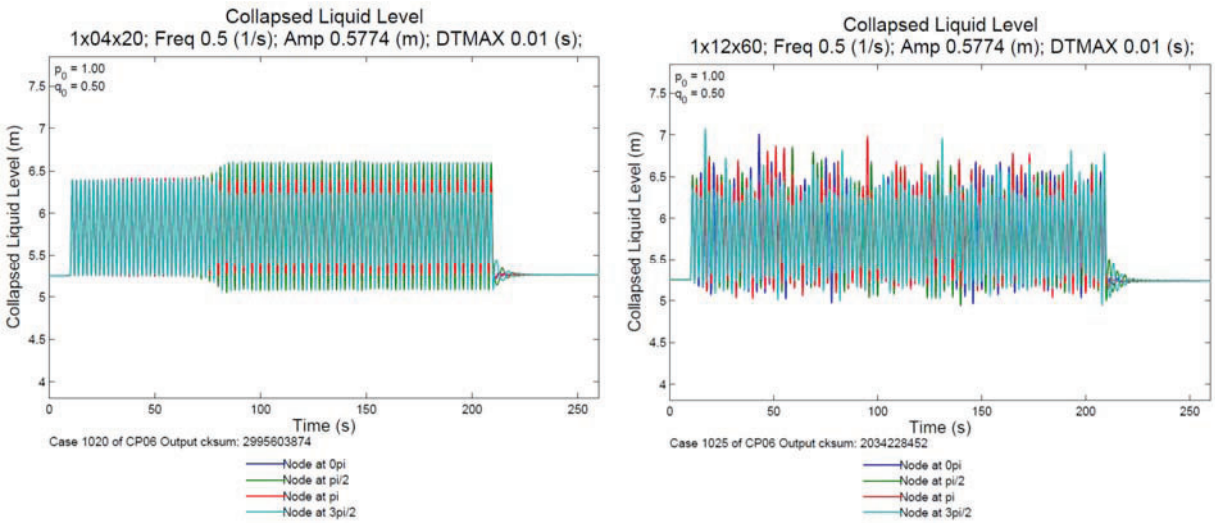

Figure 7 – Mesh sensitivity studies, predicted collapsed liquid levels

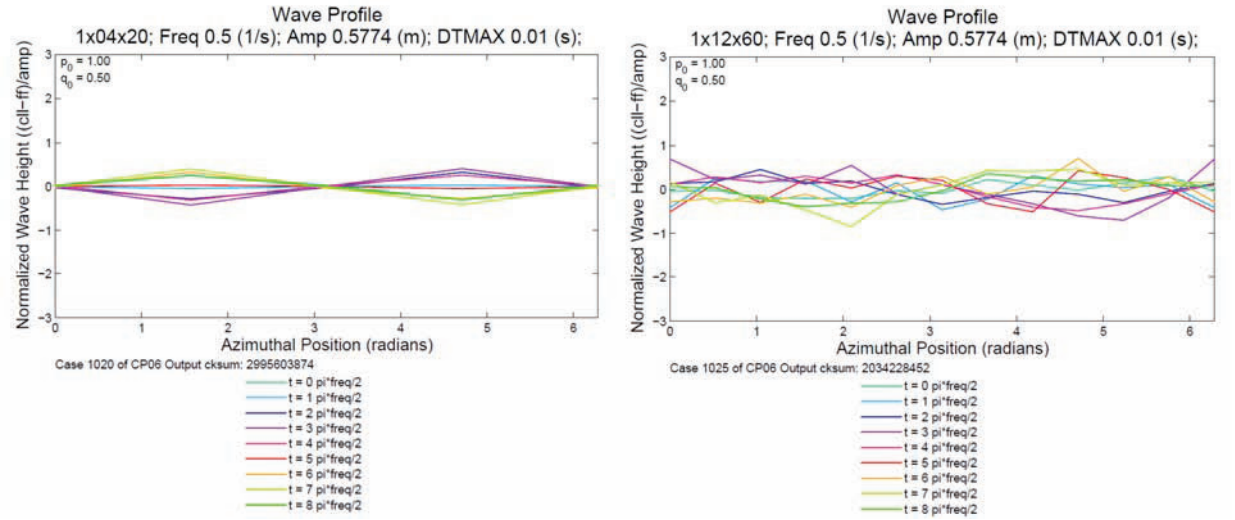

Figure 8 – Mesh sensitivity studies, Faraday wave profile

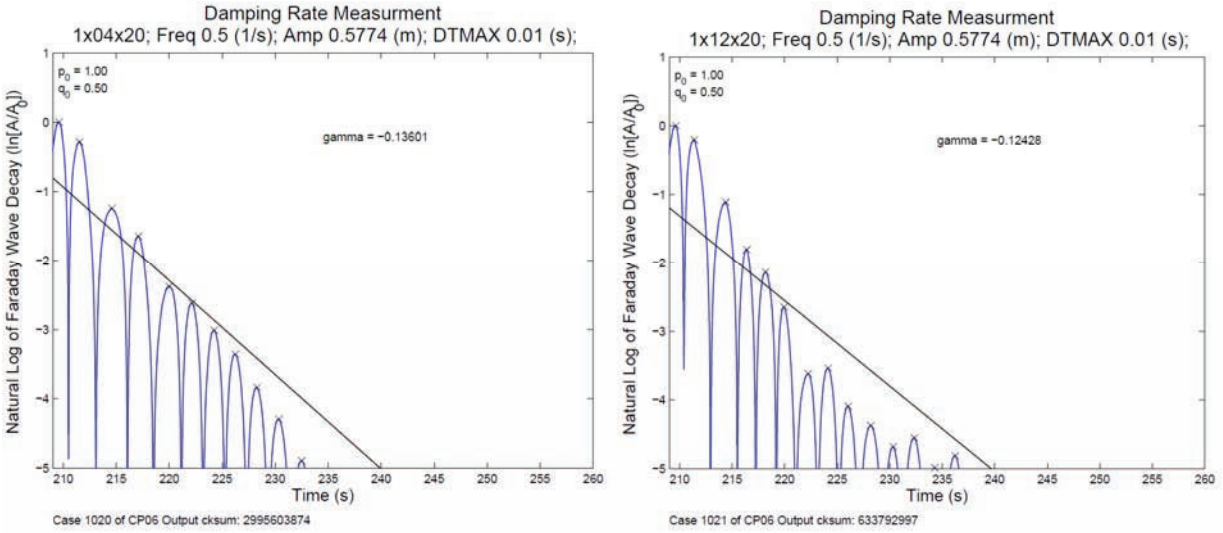

Figure 9 – Faraday wave damping factor at termination of forcing function for Cases 1020 and 1021

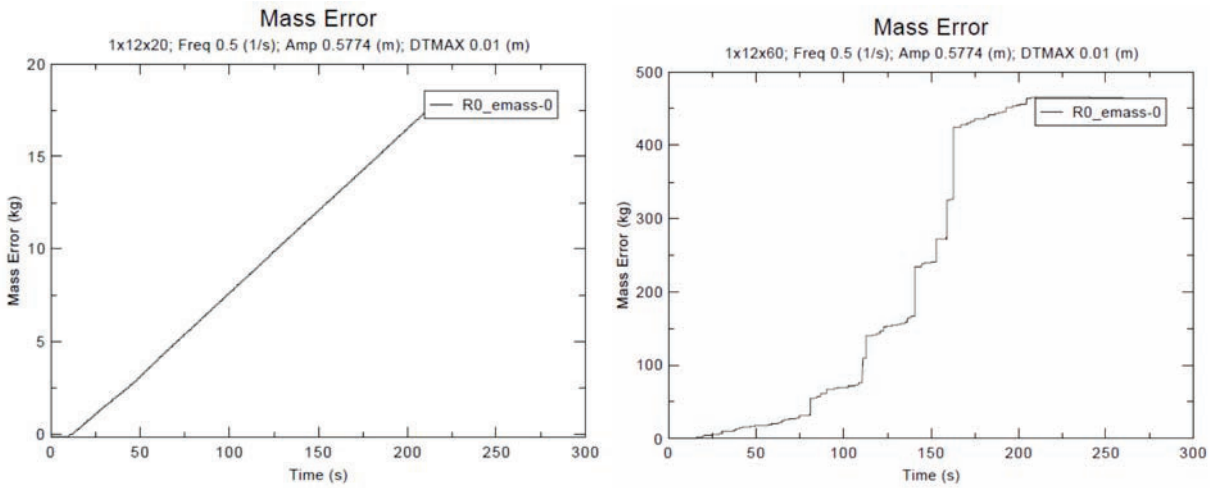

Figure 10 – Mass Error for Cases 1021 and 1025

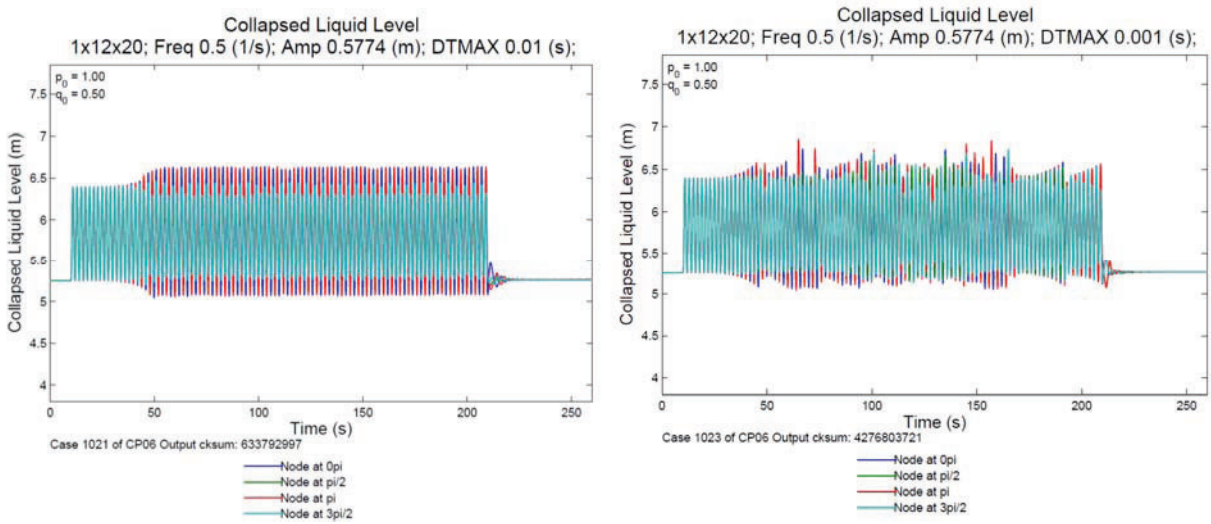

Figure 11 – Time step size sensitivity study: Case 1021 (left) and Case 1023 (right)

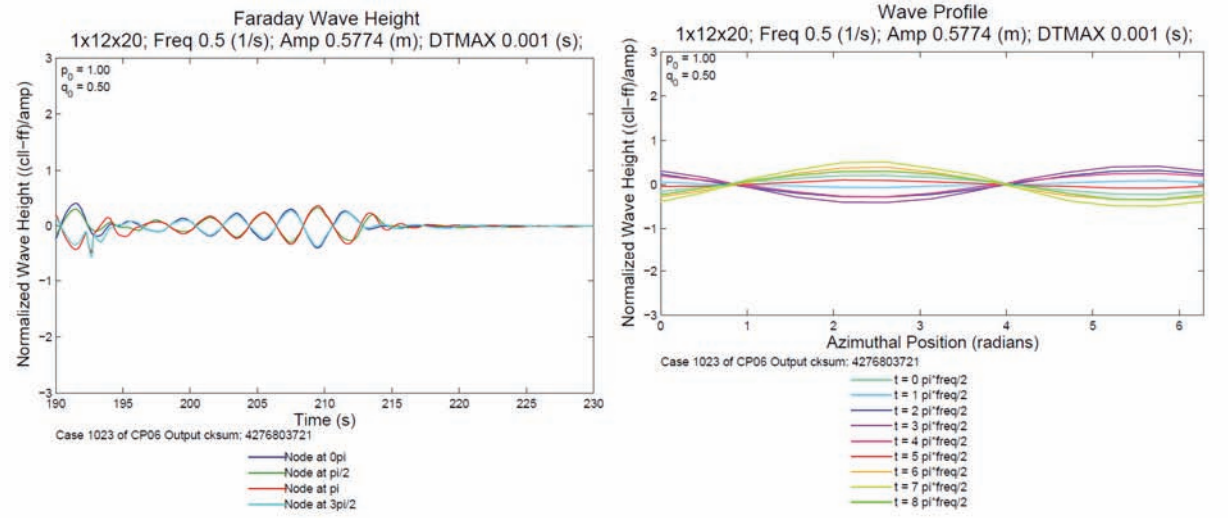

Figure 12 – Case 1023 Faraday Wave

4.2 Other Considerations

A detailed analysis of the RELAP5-3D results from the above cases indicates that the level is "smeared" in the numerical solution. Activating the level tracking function available in RELAP5-3D was found to improve this behaviour[1]. Figure 13 shows the predicted void fraction in various nodes below and above the location of the water/gas interface. The level is better defined when the level tracking option is activated as shown by the right hand plot in Figure 13.

The level definition has a significant impact on the solution. The level sharpening (level tracking) appears to destabilize the system. Figure 14 through Figure 17 shows that the critical amplitude for the sub-harmonic resonance appears to be smaller in cases with level tracking active than the equivalent cases without level tracking presented in Section 4.1. Moreover for larger amplitudes of the forcing function (A>0.5 m) the resonance is unbounded and the wave amplitude grows until the code crashes not being able to resolve the non-linear evolution and breaking of the wave motion (Figure 15 and Figure 16). The onset of instability is anticipated as the amplitude of the forcing function increases. This is an expected result consistent with an exponential growth of the instability. However without further analysis it is unclear at this point the mathematical or numerical reasons that justify this behaviour.

Figure 17 shows the result from a time step size sensitivity study conducted on the cases with the level tracking option active. The reduction of the time step size has a stabilizing effect because of the increased numerical viscosity as observed in the previous section.

[1] The option is identified in Figure 14 through 17 by the flag FF LS (Frozen Flow Level Sharpening)

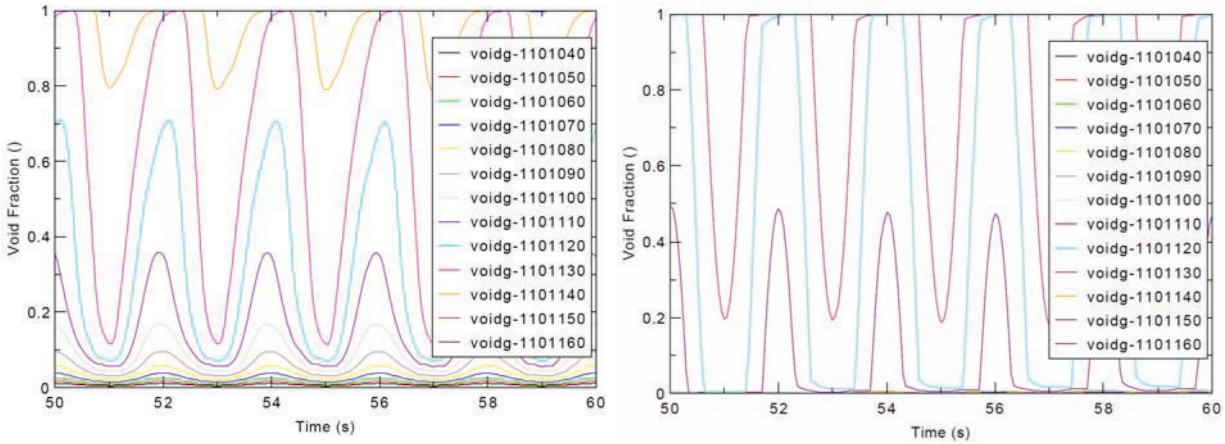

Figure 13 – Void fraction in the various nodes below and above the theoretical location of the liquid level

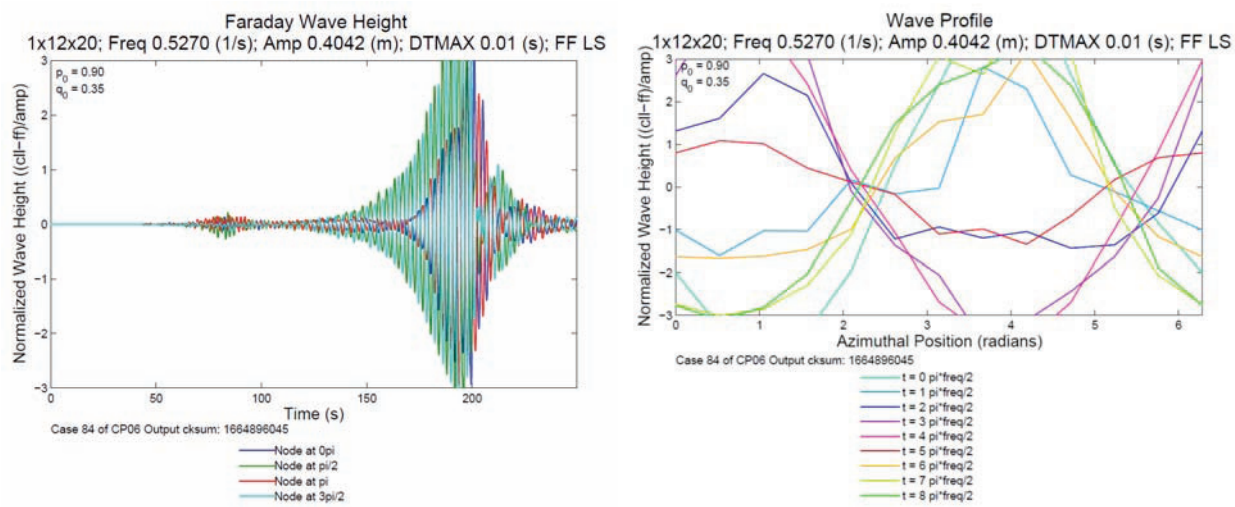

Figure 14 - Case 84: Development of Faraday wave

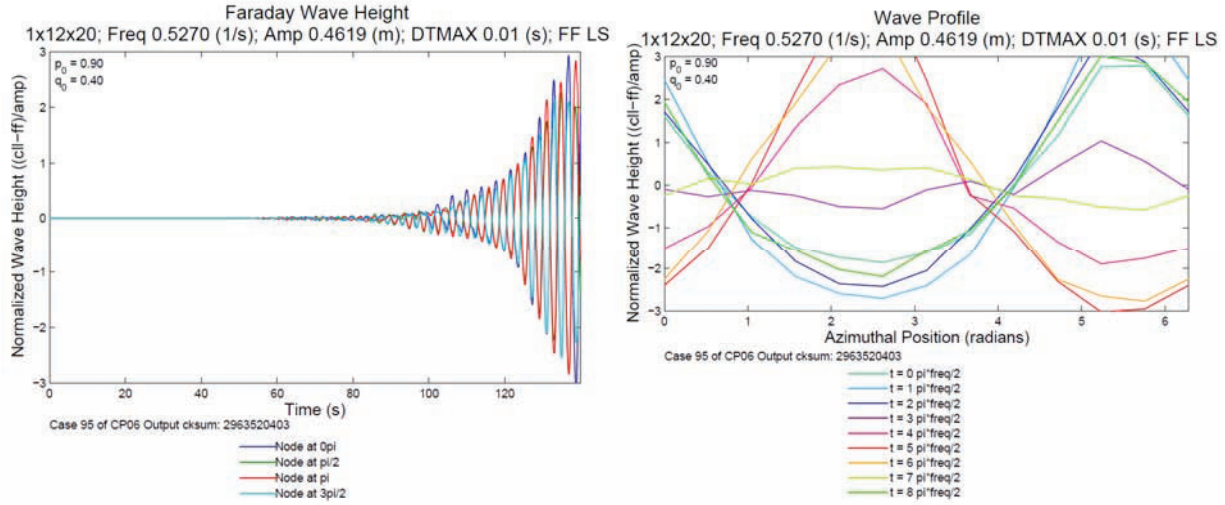

Figure 15 - Case 95: Development of an unbounded Faraday wave

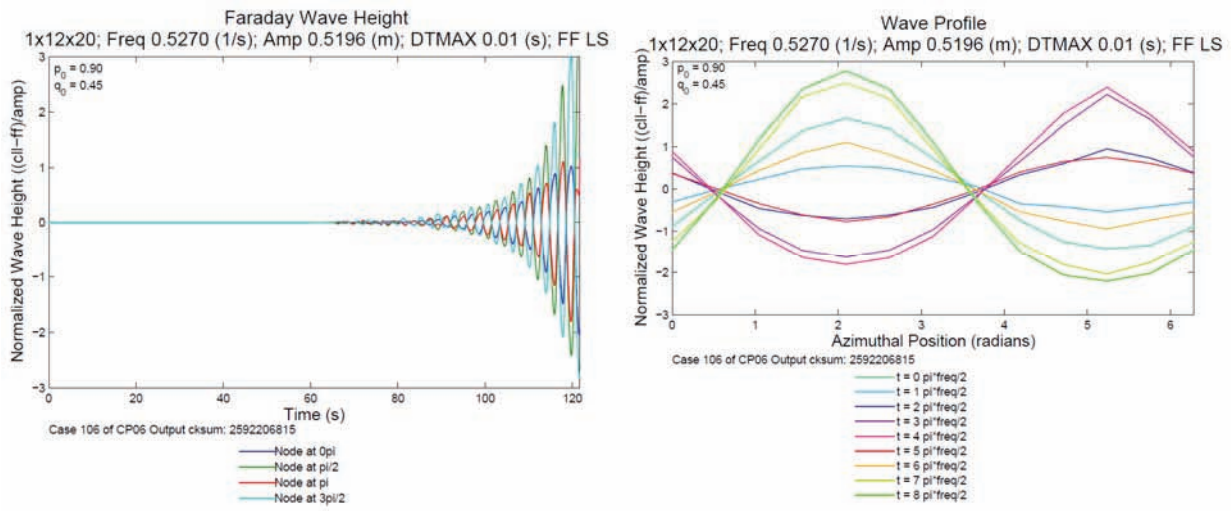

Figure 16 – Case 106: Development of an unbounded Faraday wave

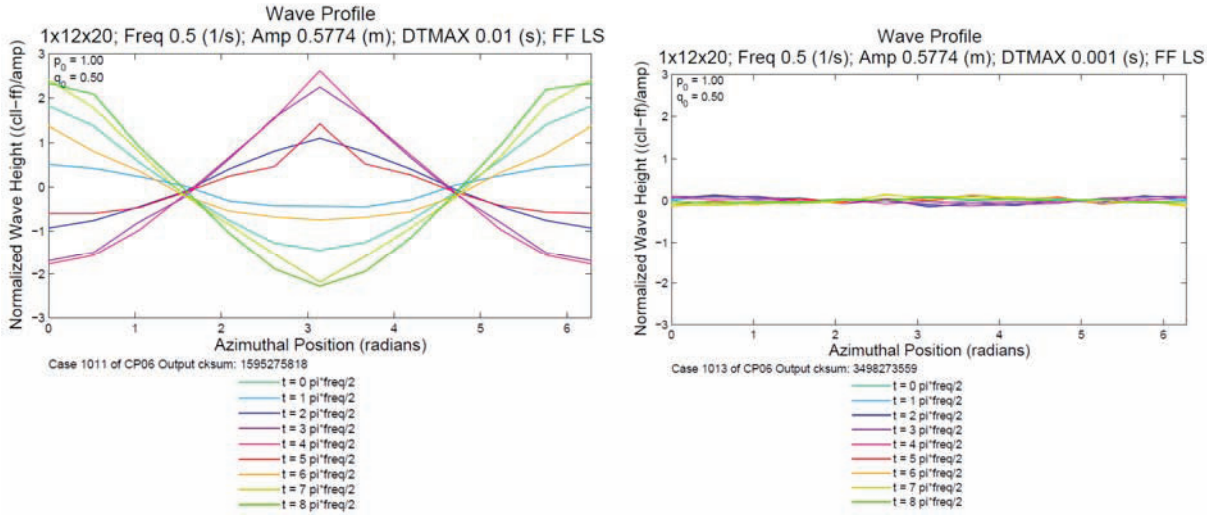

Figure 17 – Time Step Size Sensitivity on the development of a Faraday wave when the Level Tracking is active

5. CONCLUSIONS

RELAP5-3D is able to predict the development of Faraday instability and wave growth in an annular geometry which approximates the dimensions of the downcomer in the UPTF test facility. The most unstable frequency for the forcing function is shown to be slightly underestimated compared to results reported for other codes like WCOBRA/TRAC [2]. However, consistent with the previous work, the predicted critical amplitude shows a strong numerical damping effect. This is consistent with the expected level of numerical diffusion present in system codes that rely on a first order discretization of time and space.

Several studies that include the effect of mesh size, time step size and modeling options are discussed. One interesting observation is the significant impact of level tracking on the predicted stability and on the evolution of the induced Faraday waves for forcing functions with amplitudes larger than the predicted critical amplitude for the onset of the Faraday wave in sub-harmonic resonance with the forcing function.

6. REFERENCES

[1] C. Frepoli, J. Fricano, J. Yurko, F. Buschman and D. Aumiller, "On the Defintion of a Minimum Set of Requirements to Assess the Adequacy of the RELAP5-3D Multidimensional Flow Capability with Selected Canonical Problems," in *NURETH-16, Log Number 13213*, 2015.

[2] C. Frepoli and K. Ohkawa, "Numerical Dissipation and Simulation of Faraday Waves with WCOBRA/TRAC Thermal-Hydraulic Code," Pisa, September 22-24, 2004.

[3] P. D. Bayless, N. A. Anderson, C. B. Davis, P. P. Cebull, E. A. Harvego, D. A. Barber, G. A. Mortensen, D. A. Prelewicz, J. S. Baek, D. Wang, R. Beaton, L. C. Larson and J. Atchison, "RELAP5-3D Code Manual Volume III: Developmental Assessment," U. S. Department of Energy, Idaho Falls, Idaho 83415, September 2012.

[4] K. Ohkawa and C. Frepoli, "Simulation of Farday Waves in Downcomer Geometry of PWR with WCOBRA/TRAC," Tokyo, Japan, 2003.

[5] H. W. Muller, R. Friedrich and D. Papathanassiou, "Theoretical and Experimental Investigations of the Faraday Instability," *Lecture Notes in Physics,* vol. 55, pp. 230-265, 1998.

[6] P. S. Damerell and J. W. Simons, "Reactor Safety Issues Resolved by the 2D/3D Program," U.S. NRC, Washington, DC, 1993.

[7] T. B. Benjamin and F. Ursell, "The stability of the plane free surface of a liquid in vertical periodic motion," vol. 225, no. 1163 505-515, 1954.

[8] J. Mahaffy, "TRAC-M Validation Test Matrix Appendix D PIRT Plant and Scenario Descriptions," U.S. NRC, Washington, DC, 2001.

[9] S. Chandrasekhar, Hydrodynamic and Hydromagnetic Stability, New York: Dover Publications, Inc., 1961.

[10] E. Fermi and V. N. John, "Tylor Instability of Incompressible Liquids," Tecnical Information Services, Oak Ridge, Tennessee, Los Alamos, New Mexico, 1955.

[11] D. Sharp, "An Overview of Reyleigh-Taylor Instability," *Physica,* vol. 12D, pp. 3-18, 1984.

[12] H. C. Yeh and L. S. Tong, "Potetntial flow theory of a pressurized water reactor," Ann Harbor, Michigan, 1973.